Boundary Layer on a Hypersonic Sharp Cone at Small Angle of Attack

H. A. DWYER*
University of California–Davis, Davis, Calif.

The compressible, laminar boundary-layer flow over a sharp cone has been calculated for an angle of attack slightly greater than the cone half angle. The calculations have been carried out with an inviscid flow based on an asymptotic inner and outer expansion of the flowfield. The asymptotic expansion has been carried out for both first and second order in the angle of attack, and the need for the second-order results in the boundary-layer calculations has been studied. The flow conditions were chosen so that the theoretical calculations could be compared with experimental results for important boundary-layer parameters, such as heat transfer and boundary-layer thickness. The results of the investigation show that the boundary-layer equations and the second-order inviscid flow describe well the boundary-layer characteristics, and that higher-order boundary-layer influences are not important for the flow conditions studied. The most important interaction effect between the boundary layer and inviscid flow was determined to be the displacement effect.

Introduction

THE supersonic flow over sharp conical bodies at small angles of attack has long been of major interest to fluid dynamists for the following reasons: 1) The geometry makes a good re-entry vehicle because of its high lift to drag ratio at hypersonic speeds and excellent trajectory accuracy. 2) The theoretical assumption of conical inviscid flow allows for considerable simplification in analysis. 3) All conical flows have the important characteristic of three-dimensional separation. Considering the significance of the previous points, it is not surprising that there has been a large amount of effort spent on solving these types of problems. However, none of the previous analyses have made a detailed comparison between theory and experiment at hypersonic speeds, where important peculiarities such as a vortical singularity can become of importance. A major early paper on conical boundary layers was written by Moore,[1] and this article contains many of the important ideas involved in posing the boundary-layer problem. Moore showed that the transformations of independent and dependent variables used in two-dimensional boundary-layer theory were very useful in three-dimensional flows, and also set up the problem of the compressible, three-dimensional boundary-layer flow over a right circular cone at angle of attack. In another paper,[2] Moore solved the laminar boundary-layer equations along the windward and leeward line of symmetry, and showed how a crossflow derivative can influence the skin friction and heat transfer along a line of zero crossflow velocity.

After the early work of Moore, progress on understanding the flow over the body of the cone between the windward and leeward lines of symmetry was very slow, because of the lack of adequate methods of solving the equations. However, recently the use of digital computers has made it possible to solve the pertinent equations (the equations are one order of magnitude easier to solve than the full three-dimensional boundary-layer equations, since the conical nature of the flow reduces the number of independent variables to two in the transformed coordinates). A calculation of the boundary layer on a supersonic cone at angle of attack has already been carried out by Cooke.[3] Cooke has successfully calculated the flow over a cone at moderate supersonic speeds, but the inviscid solution used was only good to first order in angle of attack (this approximation of the inviscid flow could cause Cooke's calculation of the separation line to be inaccurate). Also, Cooke did not carry out calculations for the hypersonic flow case where the concentration of vorticity on the leeward side of the cone could exert an influence on the flow. Finally, the work of Cooke did not compare the results of the sharp cone calculations with any existing experimental data, such as Tracy's work.[4] Recently an investigation similar in some respects to the present one has been carried out independently by Boericke.[13]

Received January 29, 1970; revision received August 3, 1970.
* Associate Professor, Department of Mechanical Engineering. Member AIAA.

Boundary-Layer Equations

In this investigation the basic equations which will serve as the starting point of the analysis will be the three-dimensional, compressible boundary-layer equations, which are given below for the flow over a general axisymmetric body at angle of attack:

continuity

$$\frac{\partial}{\partial x}(\rho r u) + \frac{\partial}{\partial y}(\rho r v) + \frac{1}{r}\frac{\partial}{\partial s}(\rho r w) = 0 \tag{1}$$

x-momentum

$$\rho u\frac{\partial u}{\partial x} + \rho v\frac{\partial u}{\partial y} + \frac{\rho w}{r}\frac{\partial u}{\partial s} - \frac{\rho r'}{r}w^2 = -\frac{\partial P}{\partial x} + \frac{\partial}{\partial y}\left(\mu\frac{\partial u}{\partial y}\right) \tag{2}$$

s-momentum

$$\rho u\frac{\partial w}{\partial x} + \rho v\frac{\partial w}{\partial y} + \frac{\rho w}{r}\frac{\partial w}{\partial s} + \frac{\rho r' u w}{r} = -\frac{1}{r}\frac{\partial P}{\partial s} + \frac{\partial}{\partial y}\left(\mu\frac{\partial w}{\partial y}\right) \tag{3}$$

energy

$$\rho u\frac{\partial H}{\partial x} + \rho v\frac{\partial H}{\partial y} + \rho w\frac{\partial H}{\partial s} = u\frac{\partial P}{\partial x} + \frac{w}{r}\frac{\partial P}{\partial s} + \frac{1}{P_r}\frac{\partial}{\partial y}\left(\mu\frac{\partial H}{\partial y}\right) + \mu\left[\left(\frac{\partial u}{\partial y}\right)^2 + \left(\frac{\partial w}{\partial y}\right)^2\right] \tag{4}$$

where u, v, and w are the velocities in the x, y, and s directions (see Fig. 1), respectively, and H is the static enthalpy. The other quantities in the previous equations are defined as $r(x)$—local right cone radius, r'–derivative of r with respect to

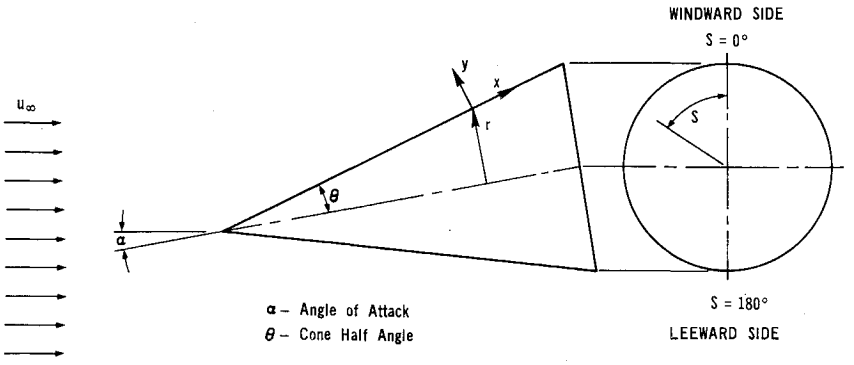

Fig. 1 Cone geometry.

x, p–boundary-layer pressure, μ–viscosity, Pr–Prandtl number, and ρ–density.

For the problem under investigation, these equations can be considerably simplified by taking advantage of the fact that the inviscid flow is conical. Moore[1] has shown that the behavior of the boundary-layer characteristics in the x direction can be described by a similarity variable which is a function of x and y. This similarity transformation will reduce the number of independent variables in the transformed equations from three to two, and thus reduce considerably the complexity of any calculation of the flow. Also, the transformation applied to Eqs. (1–4) will considerably improve the accuracy of the numerical calculations since they remove a large portion of boundary-layer growth, and also stretch the coordinates to smooth out rapid changes in the flow in the x and s directions.

The transformations which were used in the calculations are listed below:

Step I

$$\xi_1 = \int_0^x r^2 dx \quad \eta_1 = \int_0^y \frac{\rho}{\rho_\infty}\left(\frac{P_\infty}{P_1}\right)^{1/2} r\,dy \quad s_1 = s$$

Step II

$$\eta = \left(\frac{\rho_\infty u_\infty}{2\mu_\infty \xi_1}\right)^{1/2} \eta_1 \quad \zeta = s_1$$

where ρ_∞, P_∞, and u_∞ are arbitrary constant reference quantities and P_1 is the local boundary-layer pressure. The transformations in Step I are a combined Howarth and Mangler transformation, whereas Step II can be considered a modified type of Blasius transformation. The over-all effect of these transformations is to reduce boundary-layer change due to compressibility, three-dimensionality, and viscous growth. If the previous transformations are introduced into the Eqs. (1–4) and if advantage is taken of similarity in the x direction, the following set of equations result:

continuity

$$-\frac{\partial U}{\partial \eta}\frac{\eta}{6\bar{l}^2} + \frac{\phi^{1/2}}{r}\left(\frac{P_\infty}{P_1}\right)^{1/2}\frac{\partial V}{\partial \eta} + \frac{1}{3c\bar{l}^2}\frac{\partial W}{\partial \zeta} + \frac{1}{3c\bar{l}^2}\frac{\partial W}{\partial \eta}\frac{\partial \eta}{\partial \zeta} + \frac{U}{3\bar{l}^2} = 0 \quad (5)$$

x-momentum

$$\bar{V}\frac{\partial U}{\partial \eta} + \frac{W}{3c\bar{l}^2}\frac{\partial U}{\partial \zeta} - \frac{W^2}{3\bar{l}^2} = \frac{\partial}{\partial \eta}\left(\bar{l}_1\frac{\partial U}{\partial \eta}\right) \quad (6)$$

s-momentum

$$\bar{V}\frac{\partial W}{\partial \eta} + \frac{W}{3c\bar{l}^2}\frac{\partial W}{\partial \zeta} + \frac{WU}{3\bar{l}^2} = -\frac{\rho_\infty^2}{\rho}\frac{1}{3c\bar{l}^2}\frac{\partial P_1}{\partial \zeta} + \frac{\partial}{\partial \eta}\left(l_1\frac{\partial W}{\partial \eta}\right) \quad (7)$$

energy

$$\bar{V}\frac{\partial H}{\partial \eta} + \frac{W}{3c\bar{l}^2}\frac{\partial H}{\partial \zeta} = \frac{1}{\rho}\frac{W}{3c\bar{l}^2}\frac{\partial P}{\partial \zeta} + \frac{l_1}{P_\infty^2}\left[\left(\frac{\partial U}{\partial \eta}\right)^2 + \left(\frac{\partial W}{\partial \eta}\right)^2\right] + \frac{1}{P_r}\frac{\partial}{\partial \eta}\left(l_1\frac{\partial H}{\partial \eta}\right) \quad (8)$$

where the Chapman-Rubesin viscosity law has been employed and the following change of dependent variables and parameters introduced:

$$\bar{V} = \frac{\phi^{1/2}}{r}\left(\frac{P_\infty}{P_1}\right)^{1/2} V - \frac{nU}{6\bar{l}^2} + \frac{W}{3c\bar{l}^2}\frac{\partial n}{\partial \zeta}$$

$$U = \rho_\infty u, \; W = \rho_\infty W, \; l_1 = \mu T_\infty / T$$

$$\bar{l} = \left(\frac{\rho_\infty u_\infty}{2\mu_\infty}\right)^{1/2}, \quad c = \sin(\text{cone half angle}), \quad \phi = \frac{r^3}{3c\bar{l}^2}$$

The resulting set of equations in Eqs. (5–8) contains only two independent variables, and thus, the amount of effort in numerically solving these equations is considerably reduced. The mathematical nature of Eqs. (5–8) is parabolic with an initial value problem posed in ζ and a boundary value problem posed in η. This means essentially that initial conditions on U, V, W, and H must be specified at $\zeta = 0$, and boundary conditions on U, V, W, and H at $\eta = 0$ and $\eta \cong \infty$.

Inviscid Flowfield or Boundary Conditions

In order to calculate the boundary layer over a right circular cone at supersonic speeds and angle of attack, one must have accurate values for the inviscid velocities and enthalpy at the surface of the body. These values will serve as boundary conditions at the outer edge of the boundary layer, and also determine the pressure gradients in the flow. The problem of the right circular cone has been quite controversial because of the existence of a vortical singularity.[5] As a result of the vortical singularity, the work of Kopal[6] had to be reinterpreted in order for the results to apply near the leeward stagnation line. Munson[7] has successfully analyzed the vortical singularity, and has worked out a method of solution where Kopal's original tabulated work can be used.

For the problem of the boundary-layer flow over the cone at small angle of attack to be solved in this paper, the first and second-order results of Munson will be used (first- and second order refers to the first and second-order solutions which result from an asymptotic expansion of the inviscid equations in the angle-of-attack parameter). Solutions to the boundary-layer flow will be obtained for both the first- and second-order inviscid flows for angle of attack up to 12°, and the need for second-order terms evaluated.

One serious problem which resulted when the second-order tables of Kopal were used, was the complete lack of accuracy of the tables for the second-order crossflow velocity (w_1) functions at a Mach number of 8.0. In order to get around this

problem, a method of approximating the second-order crossflow velocity w_1 had to be found. The method used to obtain w_1 was to solve the inviscid crossflow momentum equation, which is given as

$$w_1(\partial w_1/\partial s) + r'u_1w_1 = -(1/\rho_1)\partial P_1/\partial s \qquad (9)$$

where u_1 and P_1 were obtained from Kopal's tables and Munson's solution (with second-order accuracy), and ρ_1 was evaluated from the equation of state and the energy equation.

Solutions to Eq. (9) were not able to be found by standard explicit numerical techniques for ordinary differential equations (Rurge-Kutta, Predictor-Corrector), because of the nonlinearity of the equation. However, by evaluating the term $r'u_1w_1$ by an implicit procedure, the finite difference method was stabilized and solutions were obtained. Another method for obtaining w_1 was to use the hypersonic flow approximation

$$w_1u_1r' = -(1/\rho_1)\partial P_1/\partial s \qquad (10)$$

As will be shown later, the boundary-layer characteristics such as skin friction, heat transfer, and displacement thickness were somewhat insensitive to the w_1 calculation. The insensitivity of the calculations to w_1 is important, since both of the methods listed previously give finite, but small, values of w_1 on the leeward line of symmetry. In general, the problem of an approximate w_1 for the second-order inviscid flow did not turn out to be a serious one.

Initial Conditions

Since Eqs. (5–8) consist basically of parabolic partial differential equations, it is necessary to have initial velocity and enthalpy profiles at $s = 0$, if the full equations are to be solved numerically. These initial conditions can be obtained from the equations resulting from taking the limit of Eqs. (5–8) as $\zeta \to 0$. In this limit $w \to 0$ but $\partial w/\partial\zeta \neq 0$, and the s-momentum equation must be differentiated with respect to ζ. The new dependent variable for Eq. (7) then becomes $\partial w/\partial\zeta$. The result of the limiting process is the following equations:

x-momentum

$$a\frac{\partial^3 f}{\partial\eta^3} + (f + bg)\frac{\partial^2 f}{\partial\eta^2} = 0 \qquad (11)$$

s-momentum

$$a\frac{\partial^3 g}{\partial\eta^3} + (f + bg)\frac{\partial^2 g}{\partial\eta^2} - b\left(\frac{\partial g}{\partial\eta}\right)^2 - \frac{2}{3}\frac{\partial g}{\partial\eta}\frac{\partial f}{\partial\eta} - \bar{c}T = 0 \qquad (12)$$

energy

$$\frac{a}{P_r}\frac{\partial^2 H}{\partial\eta^2} + (f + bg)\frac{\partial H}{\partial\eta} + au_1^2\frac{(\partial^2 f)^2}{\partial\eta^2} = 0 \qquad (13)$$

where $\partial f/\partial\eta = u/u_1$, $\partial g/\partial\eta = (\partial w/\partial\zeta)/\partial(w_1/\partial\zeta)$, T = temperature, $a = (\mu/\mu_\infty)T_\infty/T$, $b = (2/3c)(\partial w_1/\partial\zeta)/u_1$, $\bar{c} = (2/3cu_1)(R/\partial w_1/\partial\zeta P_1)\partial^2 P_1/\partial\zeta^2$, and $R = P/\rho T$.

The boundary conditions for these equations are

$$f = \partial f/\partial\eta = g = \partial g/\partial\eta = 0.0 \qquad \eta = 0$$

$$H = H_w \qquad \eta = 0$$

$$\partial f/\partial\eta = \partial g/\partial\eta = 1.0 \qquad \eta \equiv \infty$$

$$H = H_1 \qquad \eta \equiv \infty$$

In order to solve the equations the inviscid flow must be known, so that b and $\bar{c}$ may be obtained.

Equations (11–13) are tricky to solve since they are nonlinear and the boundary conditions are split. However, in recent years many methods for solving them have evolved. The method that was used in the paper was quasi-linearization developed by Bellman.[9] It was found that only five iterations were required, and this took 2 min on a 7040 IBM computer for one set of values for b and $\bar{c}$. The results of the calculation of the initial conditions will be included in the main body of the presentation of the solutions.

Numerical Methods Used

As mentioned previously, Eqs. (5–8) only contain two independent variables because of the similarity which exists in the x direction. Since there are only two independent variables, the implicit finite difference techniques developed by Blottner[10] can be used almost directly to solve Eqs. (5–8). The modifications made were the following: 1) all nonlinear terms were linearized by evaluating terms at the previously calculated station; 2) the momentum and energy equations were decoupled between ζ grid locations, also by evaluating the dependent variables at the previous stations; and 3) the continuity equation was written in an integrated form and solved numerically. The integrated form of the continuity equation was obtained from Eq. (5) as

$$V(\eta,\zeta) = \left(\frac{P_1}{P_\infty}\right)^{1/2}\frac{r}{\phi^{1/2}}\left[\frac{1}{6\bar{l}^2}\left(\eta U - \int_0^\eta U d\eta\right) + \frac{1}{3c\bar{l}^2}\frac{1}{P_1}\frac{\partial P_1}{\partial\zeta}\left(\eta W - \int_0^\eta W d\eta\right) - \frac{1}{3c\bar{l}^2}\int_0^\eta \frac{\partial W}{\partial\zeta}d\eta\right] \qquad (14)$$

This form of the continuity equation was employed because of oscillations which resulted from the numerical solution of the momentum equations. The oscillations occurred because of the linearization and decoupling which caused the inertia terms $W\partial U/\partial\zeta$, $W^2/3\bar{l}^2$, and $(W/3c\bar{l}^2)\partial W/\partial\zeta$ to be equal to zero in the first step of the calculation at $\zeta = 0$.

Accurate solutions were obtained by decreasing the step size $\Delta\zeta$ until convergence of the numerical values of U, V, W, and H was obtained. It was found that a step size of $\Delta\zeta = \pi/80$ gave converged results for the problems solved in this paper.

Flow Conditions

As mentioned previously, the calculations carried out in this paper were performed so that they could be compared directly with experimental data. The set of experimental data which was chosen to compare with was that of Tracy.[4] The conditions of the flowfield in our calculations were the following: $M_\infty = 7.3$ (freestream Mach number), $T_0 = 1360°$R (stagnation temperature), $T_w = 540°$R (cone wall temperature), $P_0 = 250$ psia (stagnation pressure), $P_r = 0.738$, and $\Theta_c = 10°$ (cone half angle). These conditions are essentially the same as the experimental tests of Tracy and will allow a good check to be made between theory and experiment.

In order to calculate the temperature distribution from the enthalpy distribution in the boundary layer, the equilibrium thermodynamic properties of air[11] were used. The Chapman-Rubesin relationship was used with the following numerical value:

$$\mu/\mu_r = 0.922T/T_r$$

where the reference was chosen at 600°R. Also, the perfect gas equation of state was applied in the analysis and calculations.

Results

The boundary-layer calculations which are presented in this paper were carried out for angles of attack up to 12°. The angle of attack was limited to this value because it was believed that separation of the boundary layer on the leeward side would substantially change the inviscid flowfield for

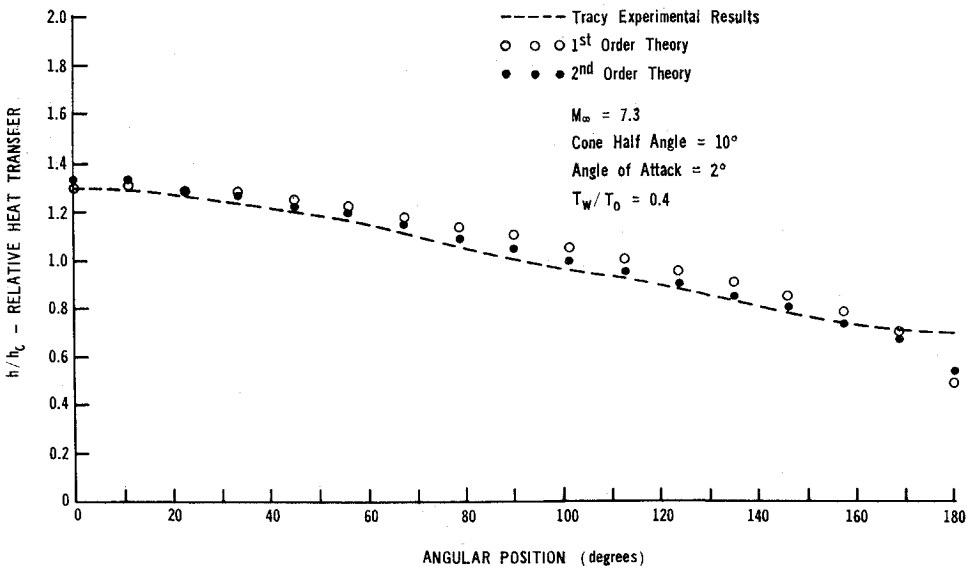

Fig. 2 Heat-transfer comparison.

angles of attack greater than this value. The experiments of Tracy were carried out for angles of attack larger than 12°; however, the results up to angles of attack of 12° will only have relevance to this paper.

The boundary-layer characteristic which was most extensively measured by Tracy was the relative heat transfer h/h_0. The reference heat transfer, h_0, was measured for the cone at zero angle of attack, with the flow conditions given previously. Figures 2–5 present a comparison of the measurements of Tracy with our theoretical calculations for angle of attack up to 8°. The abscissas of these graphs depict the angular positions on the cone with 0° and 180° being the windward and leeward lines of symmetry, respectively. In all of the figures, the results of the boundary-layer heat transfer are presented for both the first- and second-order inviscid flow boundary conditions.

Figure 2 presents the comparison of the calculations from Tracy's data for an angle of attack of 2°. As can be seen with the figure, the theoretical calculations agree well with the experimental results on the windward side for both first- and second-order inviscid flow theories. However, as the 90° position is approached, the first-order calculations begin to overpredict the heat transfer, and this seems to be the result of the pressure gradient in the S direction being too large. The second-order theory seems to do very well until the immediate vicinity of the leeward line of symmetry is reached, and then the theory underpredicts the relative heat transfer quite badly. It is difficult to explain this underprediction since the results at other angles of attack tended to overpredict the relative heat transfer (it should be expected theoretically that boundary-layer theory would overpredict leeward heat transfer and skin friction because it does not include the influence of interaction between the boundary layer and the inviscid flow). The over-all agreement between the theoretical calculations with both inviscid flows can be classified as being very good, however, even at the small angle of attack of 2° the second-order results are noticeably better. Also, it should be pointed out that the heat-transfer changes by almost 50% between the windward and leeward symmetry lines for an angle of attack of only 2°. Thus, it is seen again that a small three-dimensional effect in the inviscid flow can cause a large effect in the boundary layer.

The 4° angle of attack results are shown in Fig. 3. Again it is seen that the heat transfer calculations with the second-order theory are substantially better than the first-order results. On the windward side of the cone, there is little to choose from between the first- and second-order results, while on the leeward side the first-order theory tends to overpredict the heat transfer. The reason for this overprediction can be seen by looking at the results in Fig. 6. Figure 6 shows the experimentally measured pressure coefficient of Tracy compared with those obtained from the first- and second-order calculations [note the pressure coefficient is defined as $C_p = (P_1 - P_\infty)/(\frac{1}{2}\rho_\infty u_\infty^2)$; where the subscript ∞

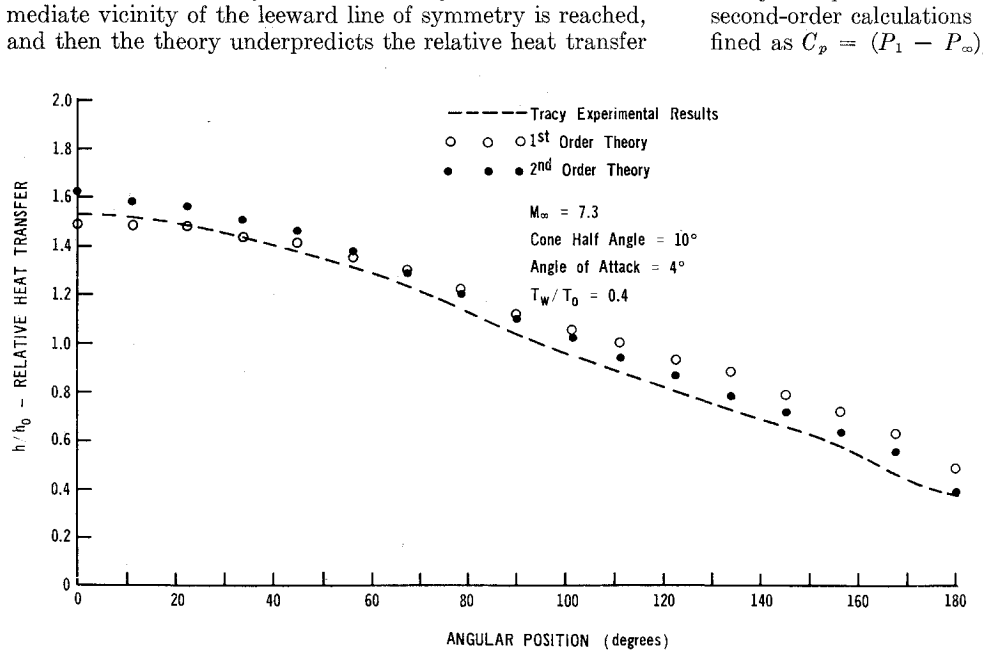

Fig. 3 Heat-transfer comparison.

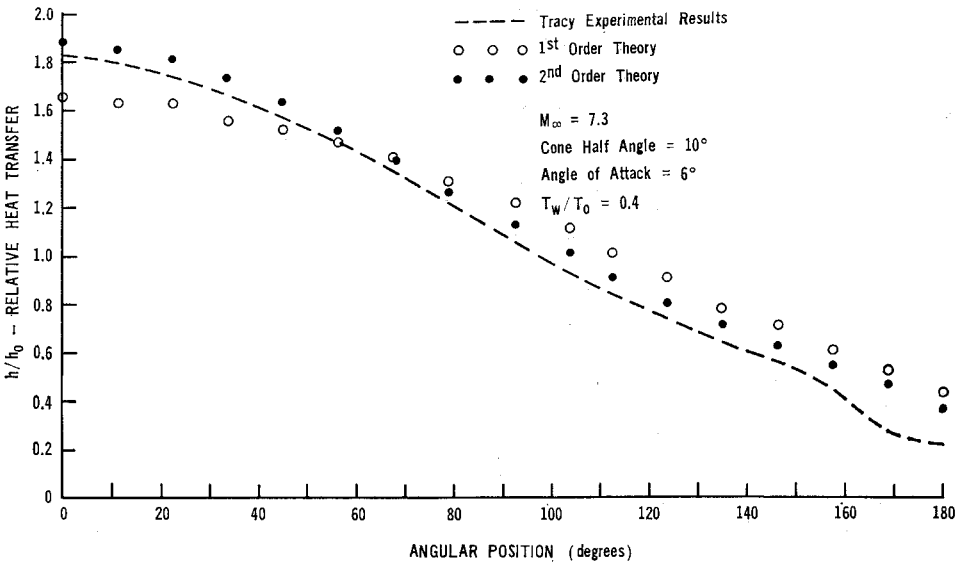

Fig. 4 Heat-transfer comparison.

refers to the uniform upstream conditions and 1 refers to the local cone body pressure]. The first-order theory tends to underpredict the leeward side pressure, thus causing a large pressure gradient. This pressure gradient is responsible for the large velocity gradients in the first-order calculations, and is also responsible for the overprediction in heat transfer.

At 6° angle of attack, the first-order theory begins to underpredict badly the windward heat transfer as shown in Fig. 4. From this result it can be said that a second-order inviscid flow calculation is necessary to adequately estimate boundary-layer characteristics for angles of attack greater than 5°. The prediction of the first-order theory seems to be reasonable on the leeward side at first glance; however, as will be shown in the 8° angle-of-attack results, the agreement is purely circumstantial.

For 8° angle of attack, it is shown in Fig. 5 that the first-order theory continues to do an inadequate job of predicting heat transfer over the majority of the body of the cone. However, the agreement near the leeward line of symmetry seems to be very good. To understand the reason for this purely circumstantial agreement, we must again look at the pressure coefficient. Figure 7 shows that the first-order pressure coefficient is bad over the entire cone body and particularly bad near the leeward line of symmetry. Why, therefore, does the heat-transfer prediction compare so well? The reason for the agreement is because of the counteracting influence of pressure gradient and low pressure. The large pressure gradient given by first-order theory at the leeward side tends to increase heat transfer, but the low pressures which result from this gradient cause a decrease in the heat transfer. The influence of pressure was especially large for this particular flow case, since the pressure on leeward side was predicted to be approximately only 4 psfa, by first-order theory, while the freestream pressure was approximately 6 psfa. The over-all result of these counteracting variables is to give a circumstantial agreement with first-order theory.

The second-order theory is seen to overpredict the leeward heat transfer at 8° angle of attack. This result is to be expected since the interaction between the boundary layer and the inviscid flow has been neglected in the calculations. This interaction tends to increase the pressure slightly at the leeward position, but at the same time decreasing the pressure gradient. The interaction at larger angles of attack eventually may cause adverse pressure gradients in the S direction.

As has been mentioned previously, the second-order inviscid flow for w_1, the crossflow inviscid velocity, is only known approximately. To test the influence of this variable on the boundary-layer calculations, a numerical experiment was performed. The experiment consisted of using the first-order inviscid crossflow velocity with the second-order pressure and radial velocity as the boundary conditions in an 8° angle-of-attack calculation. The result of this experiment was that

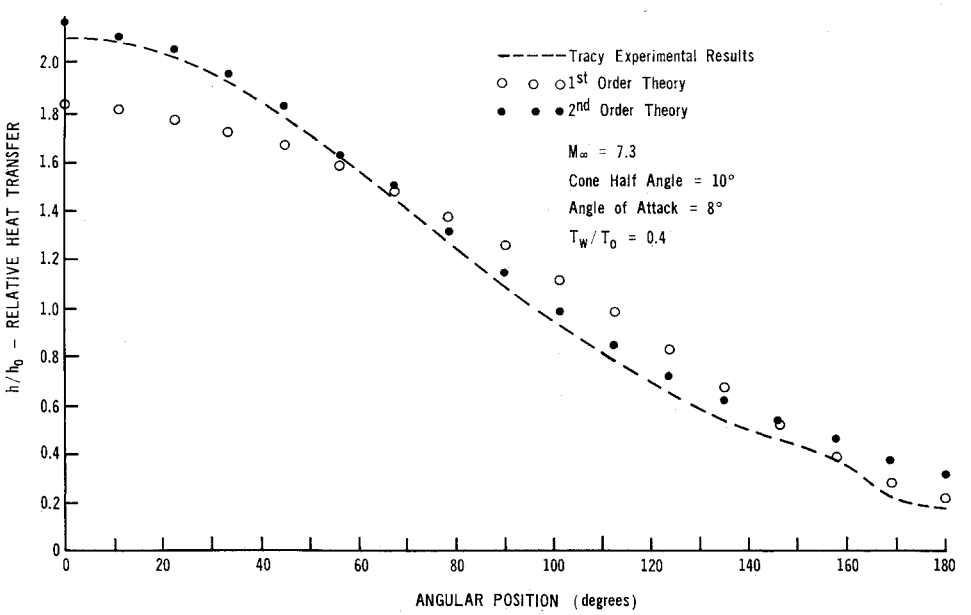

Fig. 5 Heat-transfer comparison.

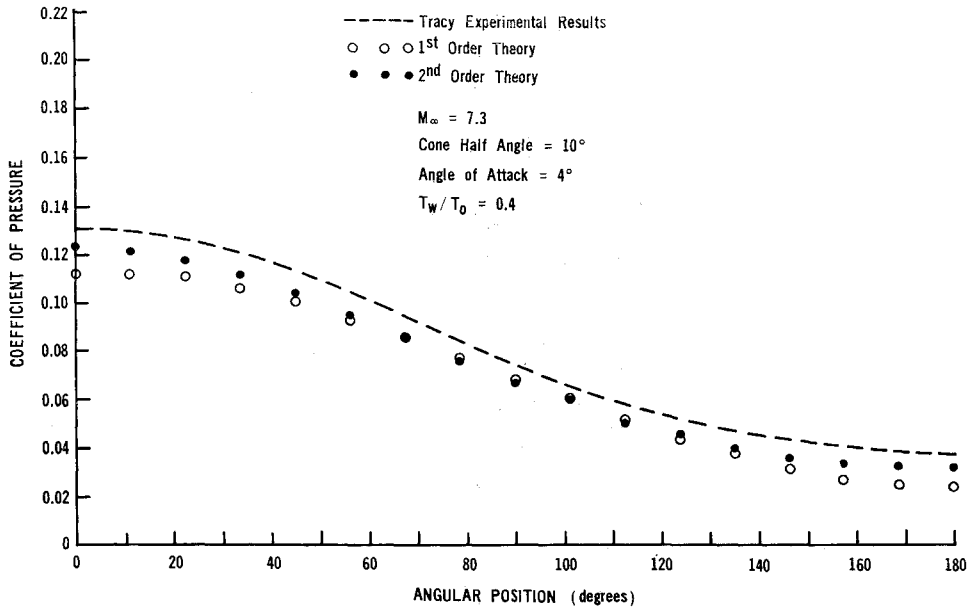

Fig. 6 Evaluation of pressure coefficient.

the relative heat transfer changed by less than 1% near the leeward symmetry line. The only conclusion that can be made from this experiment is that the pressure gradient is the more important variable in determining the boundary-layer characteristics (it should not be concluded from this discussion that crossflow does not have a large influence on the flow, since only the difference between two 8° angle-of-attack solutions have been compared).

In Fig. 8 is shown the relative heat transfer for the case of 12° angle of attack. On the windward side of the cone, the agreement between the theory and experiment is excellent. However, on the leeward side the theoretical results overpredict heat transfer in the range $90° < S < 150°$, and also predict separation at a point which does not coincide with the minimum heat-transfer location. The minimum heat-transfer point of Tracy is approximately 10° closer to the leeward symmetry line than the point of separation predicted by the boundary-layer calculation (the separation point has been defined as the S location where u, the radial component of velocity, first reversed itself in the boundary layer and was located at $S = 157°$). The fact that the theory predicts separation early is very damaging evidence for its correctness, since it would be expected that a theory which neglects displacement interactions should predict a delayed separation point. Therefore, it can be concluded that the second-order theory of Munson is not satisfactory for boundary-layer calculations where the angle of attack is larger than the cone half angle. The results in Fig. 8 do indicate, however, that the Munson method may be useful in engineering design studies in this range of angle of attack.

Tracy was not able to measure the absolute value of the heat transfer or to obtain velocity and temperature profiles in the boundary layer, therefore, some typical results will be presented. For 0° angle of attack the heat-transfer coefficient was determined to have the following value:

$$St(R_1)^{1/2}P_r = 0.558$$

where St = Stanton number and $R_1 = \rho_1 u_1 x/\mu_1$. This compares very well with that predicted by formula (8. 3.13) on p. 297 of Ref. 12, which was 0.543 (the reference quantities were chosen at 600°R for both of the previous results).

Typical temperature profiles are shown in Fig. 9 for the case of 8° angle of attack. The most interesting characteristic of the temperature profile is the large difference between the windward and leeward sides. On the windward side, the thermal boundary is very thin, whereas on the leeward side the thermal layer becomes much thicker and the temperature derivative at the wall decreases. The radial velocity profiles

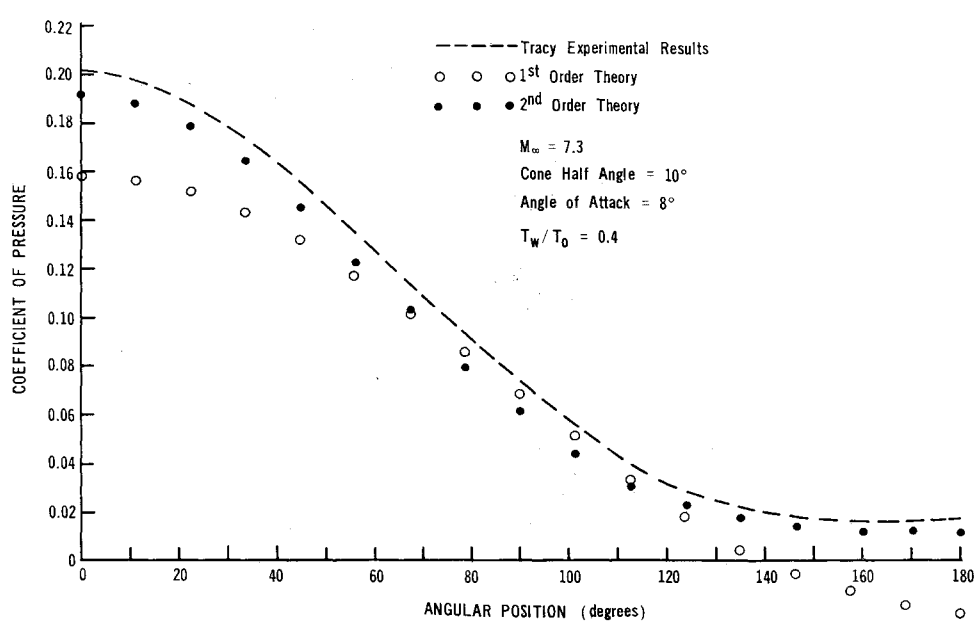

Fig. 7 Evaluation of pressure coefficient.

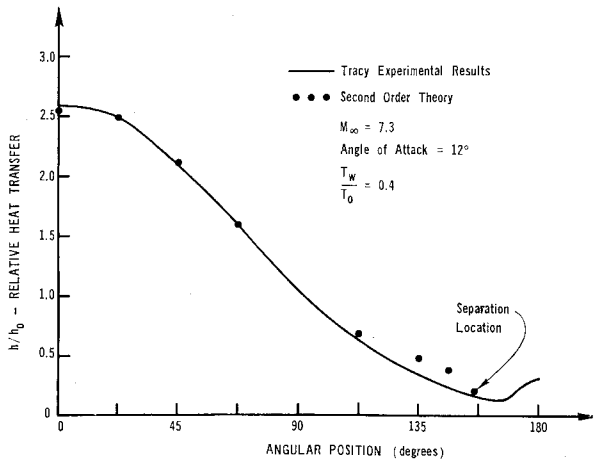

Fig. 8 Relative heat transfer.

shown in Figs. 10 and 11 exhibit essentially the same behavior as the temperature profiles. In the vicinity of the windward line, the derivative is high near the wall and the boundary-layer thickness is thin, whereas the boundary layer becomes thick and retarded near the leeward symmetry line.

Some crossflow velocity profiles are shown in Fig. 12 for the case of 8° angle of attack. The shapes of the profiles are typical of three-dimensional boundary-layer flows with the maximum crossflow velocity occurring inside the boundary layer. The crossflow velocity profile near the leeward line of symmetry has an exaggerated maximum. This maximum is a result of the approximate inviscid flow in which the pressure distribution and crossflow velocity do not exactly satisfy the inviscid equations of motion. From Fig. 12, it is seen that pressure gradient near the leeward line of symmetry is too large. The crossflow velocity profile could also be overestimated due to the lack of displacement interaction effects, which must play a role in deaccelerating the boundary-layer fluid near the leeward symmetry plane.

The final Fig. 13 presents some results of the calculation of the displacement thickness as a function of angular position around the cone (the two-dimensional definition has been used since the amount of massflow in the S direction is comparatively small). The ordinate of the figure is the ratio of the local displacement thickness (δ^*) to the displacement thickness at the windward symmetry line (δ_s^*), whereas the abscissa is the angular position on the cone. For both the 8° and 12° cases, it is seen that there is a large growth of the boundary layer near the leeward symmetry line, however, less

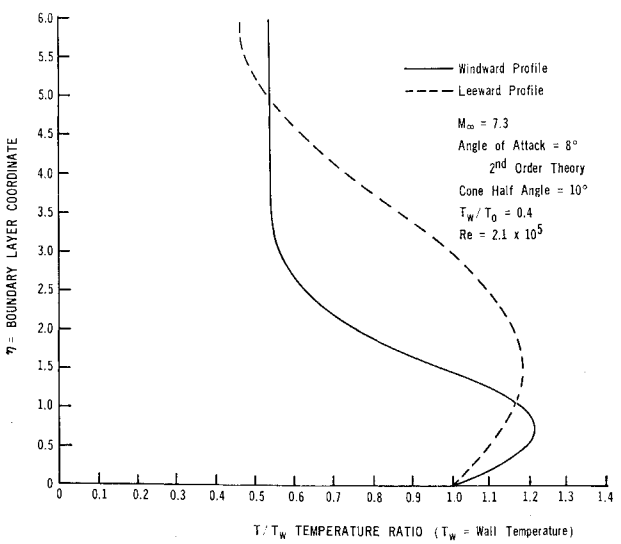

Fig. 9 Temperature profiles.

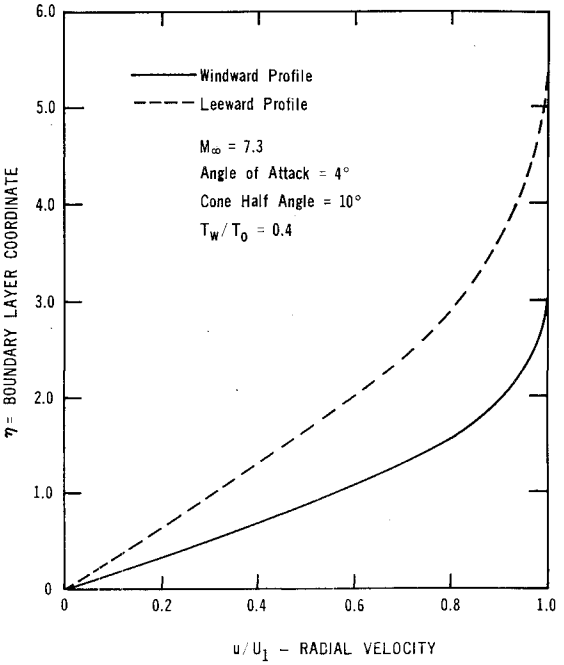

Fig. 10 Velocity profiles.

than predicted by Tracy (Tracy only measured the boundary-layer thickness and not $\delta^*)_s$. It is to be expected that the boundary-layer results should underpredict boundary-layer growth on the leeward side because of the lack of interaction influences.

The value of the displacement thickness at Tracy's measurement station 2 in. from the cone tip was found to be approximately one-third his measured boundary-layer thickness. This result seems reasonable and would also change the effective cone half angle on the leeward side roughly one-half a degree. This change in effective cone angle would cause a noticeable pressure change on the leeward side.

One final comment about the flow conditions for our calculations and Tracy's measurements is that there was a possibly slight weak pressure interaction. An estimate of the hypersonic interaction parameter $\bar{x}$, which is defined as

$$\bar{x} = M_\infty{}^3(C_\infty)^{1/2}/(Re_{x_\infty})^{1/2}$$

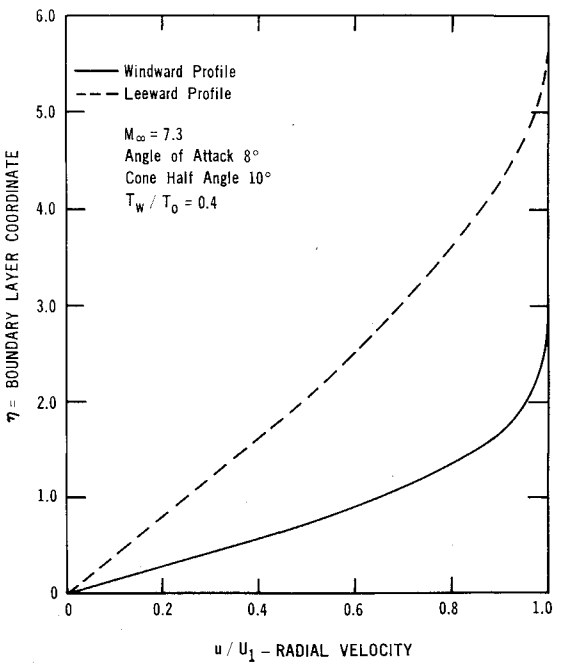

Fig. 11 Velocity profiles.

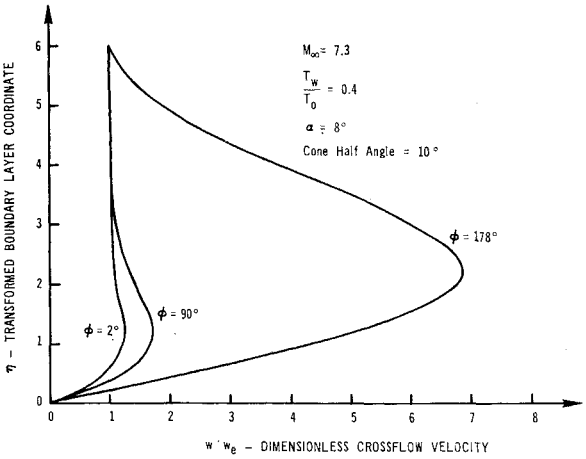

Fig. 12 Crossflow velocity profiles.

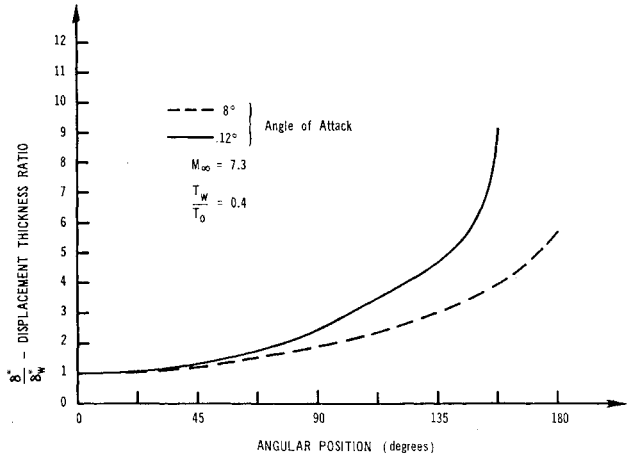

Fig. 13 Displacement thickness calculation.

at the measurement station, gave a value near 1.0. Therefore, there was a slight pressure gradient in the radial direction, which could explain the disagreement of the theory and experiment at 2° angle of attack, where the influence would be the greatest. The over-all influence of this pressure gradient, however, will be weak on the relative heat transfer around the cone.

Conclusions

1) A theoretical calculation of the boundary-layer flow around a sharp, right-circular cone at hypersonic speeds has been carried out for angles of attack up to 8°. 2) A comparison between the theoretical calculations and experimental results indicates that the boundary-layer characteristics, such as heat transfer, can be predicted well by theory for the range of angles of attack less than the cone half angle. The agreement can only be considered good when a second-order inviscid flow is used. 3) The boundary-layer calculations are noticeably more accurate for all angles of attack when the second-order inviscid flow theory is used as boundary conditions. Above 5° angle of attack, the first-order inviscid flow results give serious error. 4) In the vicinity of the leeward symmetry line, the boundary-layer flow did not seem to be sensitive to the higher-order influences of the inviscid crossflow velocity. Numerical experiments with different cross-flow velocities showed very small changes in the boundary-layer flow. 5) The boundary-layer thickness predicted by the calculations compared reasonably well with the measurements of Tracy, and it does not seem necessary to include the higher-order influence of vorticity gradients in the calculations. 6) The second-order tables of Kopal are inadequate to calculate the inviscid crossflow. However, approximate methods of predicting this inviscid crossflow velocity seem to be adequate for boundary-layer calculations. 7) For angles of attack greater than the cone half angle the boundary-layer calculations indicate that the second-order methods of Munson are inadequate as a boundary condition. The calculations indicate that the boundary-layer structure is incorrect both in a qualitative and quantitative way on the leeward side.

References

[1] Moore, F. K., "Three-Dimensional Compressible Laminar Boundary-Layer Flow," TN 2279, 1951, NACA.

[2] Moore, F. K., "Laminar Boundary Layer on Cone in Supersonic Flow at Large Angle of Attack," TR 1132, 1953, NACA.

[3] Cooke, J. C., "Supersonic Laminar Boundary Layers on Cones," R 66347, 1966, Royal Aircraft Establishment, England.

[4] Tracy, R. R., "Hypersonic Flow Over a Yawed Circular Cone," Mem. No. 69, Aug. 1, 1963, Graduate Aerospace Labs., California Institute of Technology, Pasadena, Calif.

[5] Ferri, A., Ness, N., and Kaplita, T. T., "Supersonic Flow over Conical Bodies Without Axial Symmetry," *Journal of the Aerospace Sciences*, Vol. 20, No. 8, Aug. 1963, pp. 563–572.

[6] Kopal, Z., "Tables of Supersonic Flow Around Cones," TR 1-3-5, 1947, Dept. of Electrical Engineering, Massachusetts Institute of Technology, Cambridge, Mass.

[7] Munson, A. G., "The Vortical Layer of an Inclined Cone," *Journal of Fluid Mechanics*, Vol. 20, Pt. 4, 1964, pp. 625–643.

[8] Fannelop, T. K., "A Method of Solving the Three-Dimensional Laminar Boundary Layer Equations with Application to a Lifting Body," AIAA Paper 67-159, New York, 1967.

[9] Bellman, R. E. and Kalaba, R. E., *Quasilinearization and Nonlinear Boundary-Value Problems*, American Elsevier, New York, 1965.

[10] Blottner, F., "Finite Difference Methods of Solution of the Boundary-Layer Equations," *AIAA Journal*, Vol. 8, No. 2, Feb. 1970, pp. 193–205.

[11] Keenon, J. H. and Kaye, J., *Gas Tables*, Wiley, New York, May, 1960.

[12] Hayes, W. D. and Probstein, R. F., *Hypersonic Flow Theory*, Academic Press, New York, 1959.

[13] Boericke, R. R., "The Laminar Boundary Layer on a Cone at Incidence in Supersonic Flow," AIAA Paper 70-48, New York, Jan. 1970.

[14] Reshotko, A., "Laminar Boundary Layer with Heat Transfer on a Cone at Angle of Attack in a Supersonic Stream," TN 4152, 1957, NACA.